RSC Advances

PAPER

View Article Online
View Journal | View Issue

Cite this: *RSC Adv.*, 2015, **5**, 99529

Cyclometalated iridium(III) complexes of (aryl) ethenyl functionalized 2,2′-bipyridine: synthesis, photophysical properties and *trans–cis* isomerization behavior†

Soumalya Sinha, Soumik Mandal and Parna Gupta*

Received 12th August 2015
Accepted 5th November 2015

DOI: 10.1039/c5ra16214a

www.rsc.org/advances

The syntheses, photophysical studies and photoinduced behavior of 4,4′-(aryl)ethenyl functionalized 2,2′-bipyridyls (**L1**, **L2**) and cyclometalated heteroleptic iridium(III) complexes (**1**, **2**) with **L1–L2** as ancillary ligands have been investigated in detail. The explicit characterization by time dependent ^{1}H and 2D NMR, and time dependent electronic spectra supports an expected isomerization of **L1** and **L2** from *trans–trans* configuration to *trans–cis* and *cis–cis* configurations on exposure to 366 nm UV-vis light. Interestingly, the isomerization is restricted to only *trans–cis* configuration from the existing *trans–trans* form in the ligated **L1** and **L2** of complexes **1** and **2**. The X-ray structure elucidation shows that the spatial arrangements of the (aryl)ethenyl moiety of **L2** in complex **2**, change with light exposure. The quantum chemical calculations by combined DFT-TDDFT give insight into the observed photophysical data. Furthermore, the rotational barriers of the isomerization of **L1** and **L2** were studied with variable temperature dependent ^{1}H NMR.

Introduction

Cyclometalated iridium(III) complexes with rich photophysical and electrochemical properties have a variety of applications in the field of sensors,[1] organic light-emitting diodes,[2] light-emitting electrochemical cells,[3] biological imaging agents,[4] catalysts for water splitting,[5] dye-sensitized solar cells (DSSCs)[6] and organic transformations.[7] The photophysical properties of a wide range of cyclometalated heteroleptic iridium(III) complexes with 4,4′-substituted-2,2′-bipyridyls as ancillary ligands have also been explored extensively.[1d,8] The presence of two C$^{\cap}$N ligands exhibits large ligand-field stabilization of iridium owing to its high oxidation state. In addition, strong spin orbit coupling constant of iridium ($\zeta_{Ir} = 3909\ cm^{-1}$) and long-lived triplet excited state ($\tau \sim \mu s$) enable these family of compounds to show significant photophysical properties.[8a]

The photoinduced *trans–cis* isomerization of the (aryl) ethenyl functionality is well studied and it is believed to undergo the isomerization following an excitation to the lowest triplet excited state by suitable sensitizers or to the singlet excited state by absorption of light.[9] *trans*-Stilbene and its analogues are important chromophores in many organic and organometallic materials for applications in nonlinear optics, light-emitting diodes, organic photovoltaics (OPVs), photochemical molecular devices, optical sensors, and DSSC.[10] Therefore, the study of the photoinduced *trans–cis* isomerization of the cyclometalated iridium(III) chelated with (aryl) ethenyl system is of fundamental mechanistic interest and also important for their practical applications.

Excluding Pt(II), the 5d transition metal complexes with(aryl) ethenyl substituted bipyridyl systems have not been studied extensively. Baik and Wang have reported a boron containing *trans*-stilbenoid appended 2,2′-bipyridyl ligand that undergoes *trans–cis* isomerization in the free ligand but complexation with Pt(II) prevent its isomerization.[11] However, the isomerization process of (aryl)ethenyl substituted phenyl pyridines show the isomerization process with Pt-complexes.[12] But the process of isomerization did not get enough focus in earlier reports. In this report, our objective is to understand the significant change in the photoinduced isomerization of the (aryl)ethenyl substituted 2,2′-bipyridyl ligands (**L1–L2**) in the free state, and after complexation with cationic cyclometalated iridium (**1**, **2**).

Department of Chemical Sciences, Indian Institute of Science Education and Research (IISER) Kolkata, Nadia, Mohanpur, 741246, India. E-mail: parna@iiserkol.ac.in; Fax: +91-3473279131; Tel: +91-3473279130

† Electronic supplementary information (ESI) available: Fig. S1: time-dependent ^{1}H NMR: **L2**; Fig. S2: expanded NMR: **L1**; Fig. S3: variable temperature NMR spectra **L1**, **L2**; Fig. S4: COSY and NOESY NMR spectra of **L1**; Fig. S5: time dependent electronic spectra: **L1**; Fig. S6: time-dependent ^{1}H NMR: of **2**; Fig. S7: COSY and NOESY NMR: **1**; Fig. S8: expanded ^{1}H NMR: **1** and **2**; Fig. S9: temperature dependent ^{1}H NMR of **1** and **2**; Fig. S10: time dependent electronic spectra of **2**; Fig. S11: ESI-MS of ligands **L1**, **L2**; Fig. S12: ESI-MS of complex **1** and **2**. Fig. S13: ^{13}C NMR of complexes; Table S1: selected bond distances and angles of **1** and **2**. Combined CIF. CCDC 999587, 1019401, 999588, 1050220 and 999589. For ESI and crystallographic data in CIF or other electronic format see DOI: 10.1039/c5ra16214a

It is expected that the generation of low-lying MLCT state and consequently the intramolecular energy transfer may affect the isomerization process of the (aryl)ethenyl functionality in conjugation with the iridium(III) centre.[13] Ligands were judiciously chosen to understand the steric effect on free rotation around a single bond in a five-membered *N*-methyl imidazole group, **L1** *versus* a six membered 2-methoxy phenyl group in **L2**. The ^{1}H NMR signals of methyl groups are far apart from the aromatic protons that can be easily recognized by photoinduced position changes. The ethenyl moieties photoisomerizes from *trans–trans* configuration to *trans–cis* and *cis–cis* form, when exposed at 366 nm wavelength light. On contrary the complexes **1** and **2** show only *trans–cis* form upon irradiation with the light of same wavelength. We report the detailed study of the photophysical properties and the photoinduced behavior of the iridium complexes, characterized by spectroscopic techniques and quantum chemical calculation.

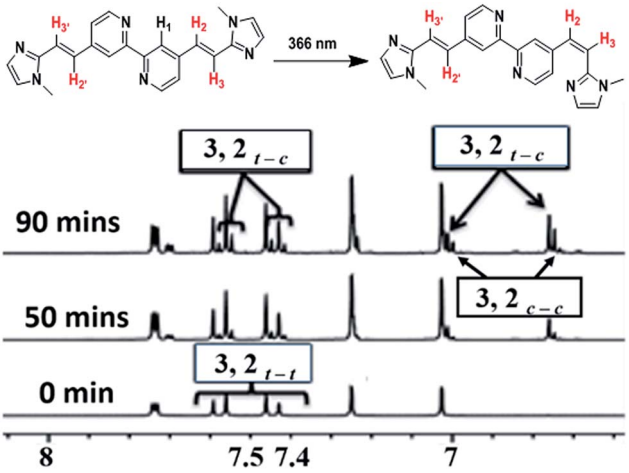

Fig. 1 Time-dependent ^{1}H NMR (DMSO-d_6, 500 MHz) spectra of **L1** under photo-irradiation.

Results and discussion

The (aryl)ethenyl appended ligands **L1** and **L2** were synthesized following the literature methods[14] by means of the Horner–Wadsworth–Emmons reaction between the appropriate aldehydes and 4,4′-diethylphosphonatomethyl-2,2′-bipyridine (Scheme 1).

We carried out all the reactions in dark condition to afford the *trans*-configuration of the (aryl)ethenyl framework. Under the dark condition (t = 0 min), AB system in ^{1}H NMR in DMSO-d_6 located at δ (ppm) 7.57; 7.44 ($^3J_{H–H}$ = 16.04 Hz) for **L1** (Fig. 1), and 7.80; 7.18 ($^3J_{H–H}$ = 16.04 Hz) for **L2** (Fig. S1†) confirm the presence of *trans–trans* (*t–t*) configuration of (aryl)ethenyl groups. However, both the ligands undergo facile olefinic *trans–cis* (*t–c*) and *cis–cis* (*c–c*) isomerization at 366 nm light exposure. Under photoirradiation, the time dependent ^{1}H NMR spectra (Fig. 1) indicate that the isomerization process for ligand **L1** reaches to the photostationary state after ~90 min (**L2** ~ 100 min) at ambient temperature. The generation of new associated peaks close to the existing peaks at δ (ppm) 7.56; 7.46 (ABq, 2H, J_{AB} = 16.04 Hz) of **L1**, and 7.73; 7.26 (ABq, 2H, J_{AB} = 16.7 Hz) of **L2** (Fig. S1†) authenticate the presence of *trans–cis* isomers. Moreover, the growth of a completely new set of peaks at δ (ppm) 6.79–6.73 (**L1**) and 6.88–6.69 (**L2**) with J_{AB} = 12 Hz describe the presence of *cis–cis* isomers. The characteristic methyl proton peak initially at δ 3.82 ppm of **L1** (Fig. S2†) and at 3.91 ppm of **L2** (Fig. S1†) gradually diminished with the growth of new peaks at δ 3.668, 3.662 ppm and 3.89, 3.78 ppm, respectively. ^{1}H NMR data further revealed that the *trans–cis* isomers contribute ~20% to the total isomerization process along with ~8% *cis–cis* isomers of **L1** and ~22% *trans–cis* isomers along with ~7% *cis–cis* isomers of **L2** at the photostationary state. The rotational barrier for **L1** is found to be ~8 kcal mol^{-1} (ref. 15) but it was difficult to calculate for **L2** due to the overlap of proton signals (Fig. S3†). However, the spectrum predicts that the rotational barrier in case of **L2** will be in the same order. Moreover, the proton couplings of **L1** and **L2** have been confirmed from the correlation diagram of ^{1}H–^{1}H COSY, ^{1}H–^{1}H NOESY NMR in DMSO-d_6 (500 MHz) (Fig. S4†).

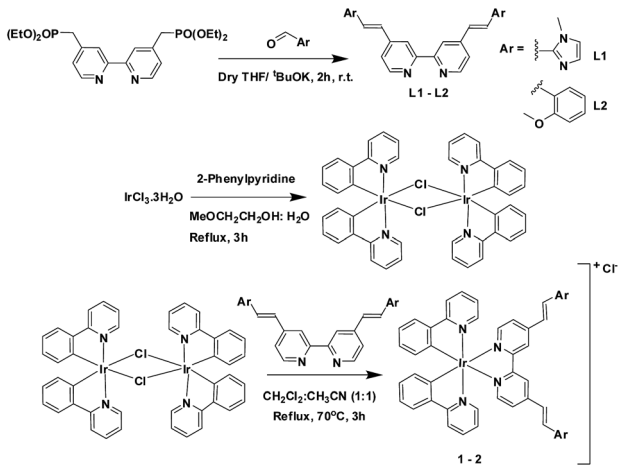

Scheme 1 Synthesis of L1–L2 and 1–2.

The structural elucidation of ligands **L1** and **L2** support the *trans–trans* disposition of the (aryl)ethenyl functionality at t = 0 min (Fig. 2). Both the ligands **L1** and **L2** possess a crystallographically imposed inversion center and the (aryl)ethenyl moieties show some deviation from planarity. The two bipyridyl rings are in the same plane with a dihedral angle between the bipyridyl and the *N*-methyl imidazolyl (**L1**, 19.83°) or 2-methoxy phenyl ring (**L2**, 13.57°). The crystallographic parameters are tabulated in Table 1 and bond parameters in Table S1.†

The ligands **L1** and **L2** dissolved in dry dichloromethane show very intense bands in absorption spectra (Fig. S5†) at λ < 400 nm ($\varepsilon \approx 8–10 \times 10^5$ M^{-1} cm^{-1}) due to spin-allowed $^1\pi$–π^* transitions and intense emission at 410 and 404 nm (Fig. 3) with quantum yield of 0.28 and 0.22 for **L1** and **L2**, respectively. The energy dissipation of light by the olefin bonds due to facile *trans–cis* and *cis–cis* isomerisation causes about 70% decrease in quantum yield of **L1** and 44% of **L2** (Table 2).

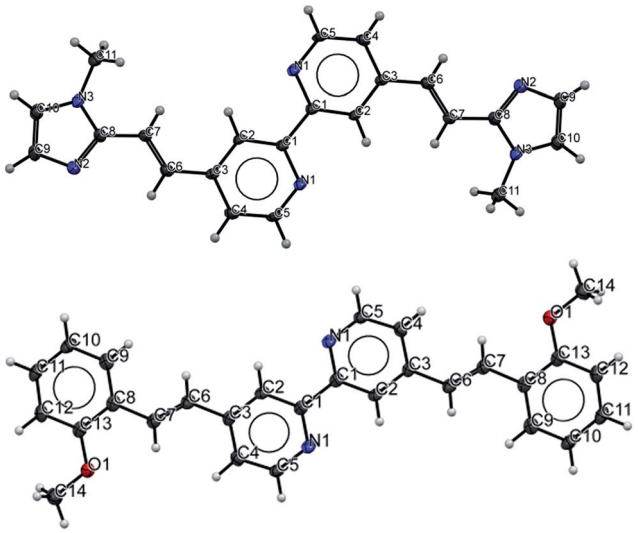

Fig. 2 ORTEP diagrams with 50% thermal ellipsoid for L1 (above) and L2 (below).

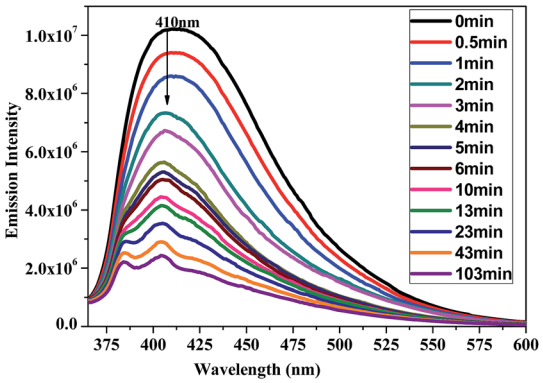

Fig. 3 Emission spectrum of 10^{-5} M L1 (λ_{ex} = 350 nm) in dry DCM under 366 nm light exposure.

Synthesis of complexes 1 and 2 (*trans*, *trans*)

The syntheses of complexes **1–2** have been done by refluxing $[Ir(ppy)_2Cl]_2$ (ppy = 2-phenylpyridine) with ligands **L1–L2** in DCM : MeCN (1 : 1) solution at 70 °C for 3 h (Scheme 1) under dark condition to avoid the *trans–cis* isomerization during the synthesis. To check the purity of the complexes, HPLC experiment (equipped with a reversed-phase column), ^{1}H and ^{13}C NMR spectroscopy were done. Both the complexes show single peak in the HPLC (Fig. S6A†) and the NMR spectra were shown

Table 1 Crystallographic parameters of L1, L2, 1, 2 and 2_{final}

	L1	L2	1	2	2_{final}
Empirical formula	$C_{22}H_{20}N_6$	$C_{28}H_{24}N_2O_2$	$C_{44}H_{36}N_8Ir$, 4($CHCl_3$), Cl	$C_{48}H_{50}N_6O_2Ir$, PF_6	$C_{50}H_{40}N_4IrO_2$,PF_6, CH_2Cl_2
Formula weight	368.44	420.49	1381.95	1066.08	1150.98
Temperature/K	100(2)	100(2)	100(2)	100(2)	100(2)
Crystal system	Mono clinic	Mono clinic	Mono clinic	Mono clinic	Mono clinic
Space group	$P2_1/n$	$P2_1/c$	$P2_1/c$	$P2_1/n$	$P2_1/n$
a/Å	8.8574(10)	12.3668(10)	10.188(9)	15.991(12)	18.773(6)
b/Å	9.1200(14)	7.3332(7)	31.26(3)	13.426(10)	13.362(4)
c/Å	12.0577(16)	12.7466(12)	17.715(16)	22.927(17)	20.727(6)
β/°	111.478(10)	113.958(11)	105.279(15)	99.761(12)	99.386(6)
Volume/Å^3	906.4(2)	1056.38(19)	5443(8)	4851(6)	5130(3)
Z	2	2	4	4	4
ρ_{calc} mg mm^{-3}	1.350	1.322	1.687	1.4597	1.490
μ/mm^{-1}	0.085	0.084	3.135	2.850	2.802
F(000)	388	444	2728	2120	2288
Crystal size/mm^3	0.05 × 0.02 × 0.01	0.31 × 0.21 × 0.12	0.42 × 0.21 × 0.12	0.18 × 0.12 × 0.04	0.38 × 0.21 × 0.08
2θ range for data collection	6.66–50°	3.6–50.02°	2.72–36.22°	1.8–33.68°	2.72–50.28°
Index ranges	$-7 \le h \le 10$, $-6 \le k \le 10$, $-12 \le l \le 13$	$-14 \le h \le 11$, $-8 \le k \le 8$, $-12 \le l \le 15$	$-7 \le h \le 8$, $-27 \le k \le 27$, $-15 \le l \le 15$	$12 \le h \le 10$, $10 \le k \le 10$, $18 \le l \le 18$	$-22 \le h \le 22$, $-13 \le k \le 15$, $-24 \le l \le 18$
Reflections collected	2106	3388	12 296	7429	36 450
Independent reflections	1414 [R_{int} = 0.0330]	1867 [R_{int} = 0.0577]	3718 [R_{int} = 0.1357]	2704 [R_{int} = 0.1050]	8987 [R_{int} = 0.1579]
Data/restraints/ parameters	1414/0/128	1867/0/146	3718/0/333	2704/9/212	8987/0/606
GOF on F^2	0.963	1.104	1.029	1.018	0.914
Final R indexes [$I \ge 2\sigma(I)$]	R_1 = 0.0628, wR_2 = 0.1457	R_1 = 0.0539, wR_2 = 0.1484	R_1 = 0.0678, wR_2 = 0.1646	R_1 = 0.0701, wR_2 = 0.1898	R_1 = 0.0679, wR_2 = 0.1428
Final R indexes [all data]	R_1 = 0.0964, wR_2 = 0.1659	R_1 = 0.0680, wR_2 = 0.1620	R_1 = 0.1167, wR_2 = 0.1988	R_1 = 0.1125, wR_2 = 0.1967	R_1 = 0.1464, wR_2 = 0.1665
Largest diff. peak/ hole/e Å^{-3}	0.31/−0.34	0.28/−0.29	1.58/−1.10	1.25/1.1	1.61/−0.92

Table 2 Photophysical parameters of L1–L2 and 1–2

Compound	λ_{Abs} ($\varepsilon \times 10^{-4}$, M^{-1} cm^{-1}) (experimental)	Calculated λ_{Abs}[a] (nm, force constant, main transition[f])	Emission (nm)	Luminescence lifetime (nS μS^{-1})	Quantum yield: Before irradiation	Quantum yield: After irradiation
L1	343(80.0) 299(16.0) 286(6.0)	346.0 ($f = 1.6388$, H−1 → L+1) 304.39 ($f = 0.1510$, H−1, H−2 → L+1) 291.03 ($f = 0.1226$, H−1, H−2 → L+1)	410 ($\lambda_{ex} = 350$)	$\tau_1 = 0.5$ (88.1%) $\tau_2 = 1.09$ (11.9%) $\chi^2 = 1.17$	0.28	0.09
L2	336(10.0) 306(69.0) 291(82.0) 282(80.0)	335.44 ($f = 0.9779$, H−1 → L) 321.21 ($f = 0.6485$, H → L+1) 294 ($f = 0.1199$, H−2 → L) 280 ($f = 0.2909$, H−3 → L)	404 ($\lambda_{ex} = 350$)	$\tau_1 = 0.08$ (93.9%) $\tau_2 = 2.43$ (6.08%) $\chi^2 = 1.17$	0.22	0.12
1	468(34.0) 390(50.0) 348(44.0) 304(41.0)	465 ($f = 0.3036$, H−1 → L) 384 ($f = 0.9313$, H−2 → L+1, H−1 → L) 358 ($f = 0.2706$, H−4 → L+1)	409 ($\lambda_{ex} = 350$) 556[b], 620[b] (541[c], $\lambda_{ex} = 410$) 568[d], 628[d,e] ($\lambda_{ex} = 410/480$)	8.39 μS[b] 38.49 μS[e]	0.32	0.10
2	470(30.0) 381(63.0) 295(83.0) 272(90.0)	467.74 ($f = 0.2017$, H−1, H−2 → L) 383.90 ($f = 0.3489$, H−2 → L+1, L+2)	406 ($\lambda_{ex} = 350$) 561[b] (564[c], $\lambda_{ex} = 410$) 545[d], 605[d,e] ($\lambda_{ex} = 410/480$)	6.34 μS[b] 24.21 μS[e]	0.26	0.05

[a] With n states = 30, we could not go beyond 330 nm. [b] Room temperature. [c] Calculated emission. [d] Solid state (thin film of dichloromethane solution on glass plate). [e] 77 K. [f] H = HOMO; L = LUMO.

in Fig. S7–S10.† The results confirm the presence of pure *trans*, *trans* form for both complexes.

NMR studies of photoirradiated complexes 1 and 2

At $t = 0$ min (in dark, *trans*, *trans*), the peaks with AB pattern (*trans*, *trans*) around the ethenyl bonds of **1** and **2** (Fig. 4) appeared at δ (ppm) 8.16; 7.47 ($^3J_{H-H} \approx 15.75$ Hz) (Fig. 5) and 7.99; 7.65 ($^3J_{H-H} \approx 16.8$ Hz) (Fig. S8†) respectively in ^{1}H NMR spectra. Under photoirradiation both the complexes experienced restricted isomerization processes that are prominent from the generation of new peaks in time dependent ^{1}H NMR spectra. All significant changes are tabulated in Table 3. The time dependent ^{1}H NMR, ^{1}H–^{1}H COSY and ^{1}H–^{1}H NOESY experiments of the complexes provide strong evidence of the presence of only *trans–cis* configuration along with the *trans–trans* configuration of ethenyl groups, once exposed to light (Fig. S7–S9†). The *cis–cis* configuration at both the sides of the bipyridyl ring has never formed. ^{1}H NMR data further revealed that the *trans–cis* isomers contribute ~30% to the total isomers for **1** and around 50% for **2** at the photostationary state. We have

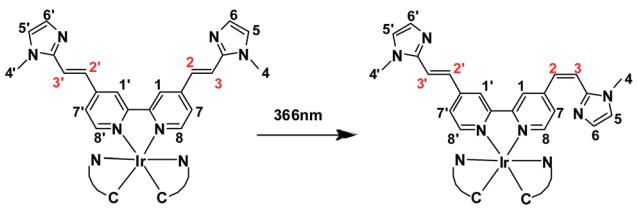

Fig. 4 C^Ns are ppy ligands. The protons of ppy are omitted for simplicity as they are not affected under photoirradiation.

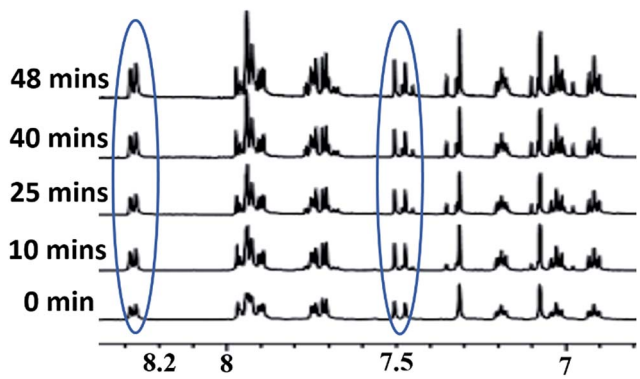

Fig. 5 Time-dependent ^{1}H NMR (DMSO-d_6, 500 MHz) spectra of **1** under photoirradiation. AB patterns are circled in the picture.

tried to calculate the rotational barrier from variable temperature ^{1}H NMR spectrum, but could not succeed due to the complicated nature of the same. The overlap of the aromatic proton signals from phenylpyridines is responsible for the complication (Fig. S11†).

X-ray crystallography

It is noteworthy that the complex **1** gets crystallized with the same *trans–trans* disposition (Fig. 6) of ethenyl groups before and after irradiation. Several attempts to grow good quality crystal were done but the quality of the crystal remains very poor in all the cases. Incidentally, after photoirradiation significant rotation around the single bond is observed in case of complex **2** (apart from the *trans–cis* isomerization). The X-ray

Table 3 The peak positions of ^{1}H NMR of complexes **1** and **2** before and after photoirradiation

Complex **1** (δ in ppm)		Complex **2** (δ in ppm)	
Initial positions	New and/or associate positions	Initial positions	New and/or associate position
H1: 9.57	9.05, 9.74	H1: 9.64	9.35, 9.19
H2: 8.22[a]	6.98[b]	H2: 7.65[c]	6.28–6.25[d]
H3: 7.47[a]	6.78[b]	H3: 7.99[c]	6.28–6.25[d]
H4: 3.90	3.84, 3.76	H4: 3.88	3.89, 3.73
H5: 7.29	7.34, 7.31	H5: 7.70	[a]
H6: 7.06	7.07, 7.09	H6: 7.58	[a]
H7: 7.85	8.78	H7: 7.51	[a]
H8: 7.74	7.68	H8: 7.02	[a]
[a]$J_{H-H} \approx 15.75$ Hz		H9: 7.76	[a]
[b]$J_{H-H} \approx 13.25$ Hz			H10: 7.90 [a]
[c]$J_{H-H} \approx 16.8$ Hz			[d]$J_{H-H} \approx 12.20$ Hz

[a] The newly generated peaks are very closely associated and could not be assigned properly.

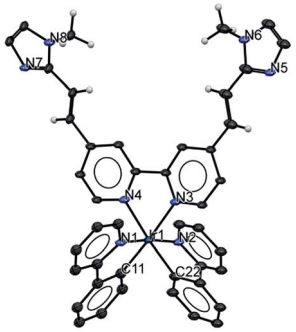

Fig. 6 X-ray crystal structure of complex **1** (50% thermal ellipsoid).

crystallographic structures of complex **2** obtained from slow diffusion of dichloromethane solution (with added NH_4PF_6) before and after the irradiation (**2** and $\mathbf{2_{final}}$) (UV-light of 366 nm) (Fig. 7), always provides different disposition of ethenyl groups. The $\mathbf{2_{final}}$ structure is the most stable structure and it is

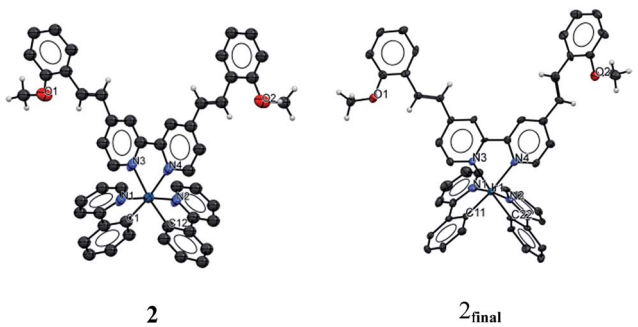

2 $\quad$ $\mathbf{2_{final}}$

Fig. 7 ORTEP diagrams with 50% thermal ellipsoid of **2** before (**2**) and after ($\mathbf{2_{final}}$) photoirradiation. Hydrogen atoms of ppy and bipyridine moieties, solvent molecules and counter anions are omitted for clarity.

also evident from the DFT study (see later). For all the cases, the *cis*-[Ir(C$^\cap$N)$_2$(N$^\cap$N)] complexes were in slightly distorted octahedral geometry in which Ir–C(ppy), Ir–N(ppy) and Ir–(N$^\cap$N) bond distances are comparable to the previously reported complexes.[16]

The light exposed complexes are thermally switchable to the initial state once heated at 70 °C in DCM : MeCN (1 : 1) solution under dark. The crystallographic parameters are tabulated in Table 1 and bond parameters in Table S1.†

Photophysical studies of complexes 1 and 2 (pure *trans*, *trans* form)

The photophysical studies of the complexes were done with the complexes with *trans*, *trans* configuration.

The absorption spectra of the cyclometalated iridium(III) complexes usually witness metal-to-ligand charge transfer (MLCT), where an electron is promoted from a metal d orbital to a vacant π^* orbital on one of the ligands, and ligand-centered (LC) transitions in which an electron is promoted from π orbital on one of the coordinated ligands. Absorption spectra (Fig. 8, Table 2) of the complexes **1** and **2** were recorded in dry DCM and dominated by intense high energy bands around 300 nm with $\varepsilon \approx 5 \times 10^5$ M^{-1} cm^{-1}, assigned to spin allowed ligand-centered ^{1}IL transitions ($^1\pi \rightarrow \pi^*$) from both the ppy and bpy ligands.[17] The moderately high energy absorption shoulders with high extinction coefficients around 382–390 nm have been assigned to an admixture of spin-allowed metal-to-ligand charge transfer (^{1}MLCT), dπ–π^*(bpy) and ligand-to-ligand charge transfer (^{1}LLCT), π(bpy)–π^*(bpy) processes (Table 2).[18] The low intensity band ($\varepsilon \approx 8 \times 10^3$ M^{-1} cm^{-1}) around 470 nm is due to the spin-forbidden transitions owing to ^{3}MLCT and ^{3}LLCT/^{3}LC transitions. The emission spectra of **1** and **2** (10 μM, dry DCM) showed λ_{max} at 406 nm (Fig. 8) and 408 nm for **1** and **2** (Fig. S12†) respectively, when excited at 350 nm. The excitation at 410 nm shows the ^{3}MLCT/^{3}LC based emission at 556 nm (620 nm, vibronic progression) and 561 nm for the complexes **1** and **2** (Fig. 8), respectively. The emission spectrum of the complex **1** show λ_{max} at 556 nm with vibronic progression at 620 nm, but such feature is absent in the case of **2**.

The solid-state emission was done with thin film of dichloromethane solution on glass. The complex **1** exhibits bright orange emission with an intense, significantly red shifted band at 568 nm with lower energy vibronic progression at 628 nm (room temperature; λ_{max}: 556 nm and 620 nm). However, in case of the complex **2**, significant blue-shifted emission at 544 nm with vibronic progression at 606 nm (room temperature; λ_{max}: 561 nm) is observed. In both the cases, at low temperature alteration of the λ_{ex} from 410 nm to 480 nm provides well resolved spectra (Fig. 8). At 77 K, the PLQY is difficult to measure with acceptable accuracy but the observed lifetime can provide quantitative information. The main emission peak of both the complexes exhibit bi-exponential decay pattern with a long excited state lifetime of 38.49 μS and 24.21 μS in the solid state. These observations confirm that the emissive center owns a triplet character and the long excited state lifetime also support that the emission

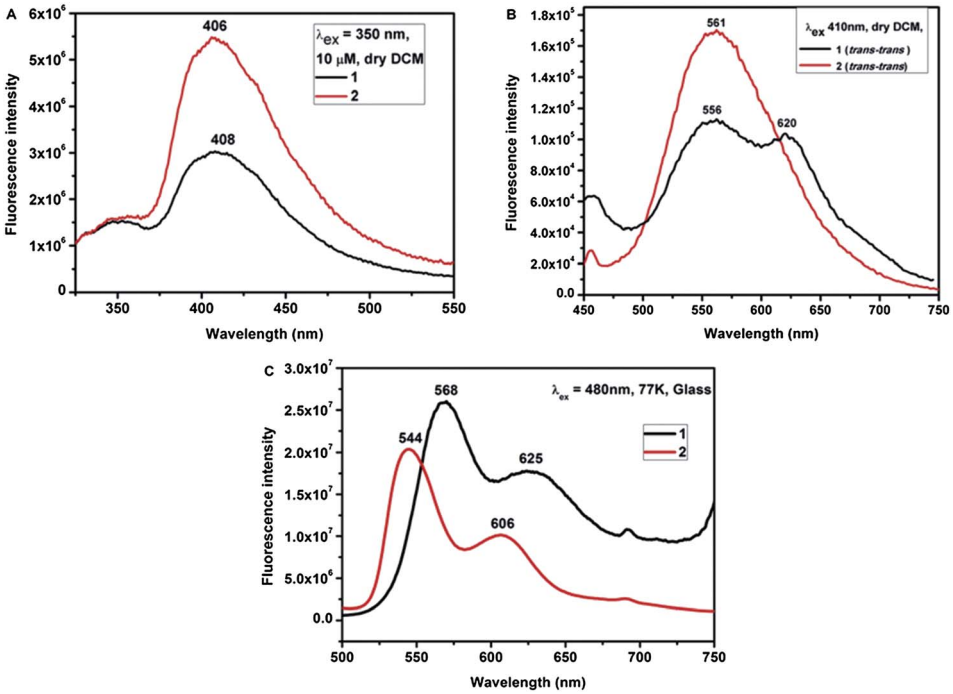

Fig. 8 The emission spectra of complexes **1** and **2** in dichloromethane solution at room temperature (A) (λ_{ex} = 350 nm) (B) (λ_{ex} = 410 nm). (C) Solid state (thin film on glass) (λ_{ex} = 410 nm/480 nm).[19]

originates from a ^{3}MLCT/^{3}LC excited state. The significant red or blue shift in the λ_{max} of the complexes attributes to the changes in the intermolecular π–π interactions by aggregation in the solid state. Strong spin–orbit coupling from the iridium(III) center facilitates intersystem crossing to energetically similar triplet states and enables the formation of an emissive mixed (triplet) excited state. This vibronic structure indeed supports considerable contribution of ^{3}LC character to the emission. To confirm the contribution of ^{3}LC character, we recorded the emission in the solid state (thin film on glass, Fig. 8). To understand the nature of emission more precisely, theoretical studies have also been done.

Photoirradiation at 366 nm

The emission intensity diminished slowly upon irradiation with ultraviolet light (λ = 366 nm). Comparison of the λ_{em} at around 406 nm of the complexes with the ligands (Table 2) indicates the ligand-based character of the emission at the said wavelength. It was noted that the complexes **1** and **2** reached at the photo stationary states after 48 and 42 minutes, respectively at ambient temperature. This signifies that the energy is dissipated through non-radiative processes. As discussed, the excitation at 410 nm before irradiation shows the ^{3}MLCT/^{3}LC based emission at 556 nm (620 nm, vibronic progression) and 561 nm for the complexes **1** and **2** (Fig. 9) and the emission of the complex **1** show λ_{max} at 556 nm with vibronic progression at 620 nm (**2**, λ_{em} = 561 nm). The emission spectra after photoirradiation showed similar pattern with reduced emission intensity (complex **1**: 546 nm, 624 nm; complex **2**: 568 nm) (Fig. 9). The mixture of isomers obtained could not be separated by column chromatography.

To separate the isomers of complexes **1** and **2** after irradiation, we tried HPLC equipped with a reversed-phase column. The mobile phase was a gradient of H_2O and acetonitrile (50%

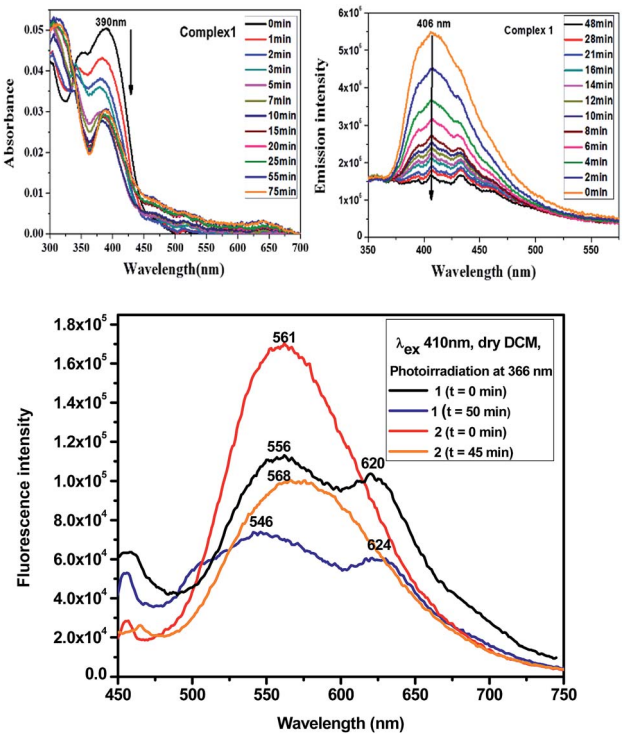

Fig. 9 Time dependent absorption (left) and emission (λ_{ex} = 350 nm) (right) spectra of **1** (10 μM) in dry DCM under 366 nm light exposure.

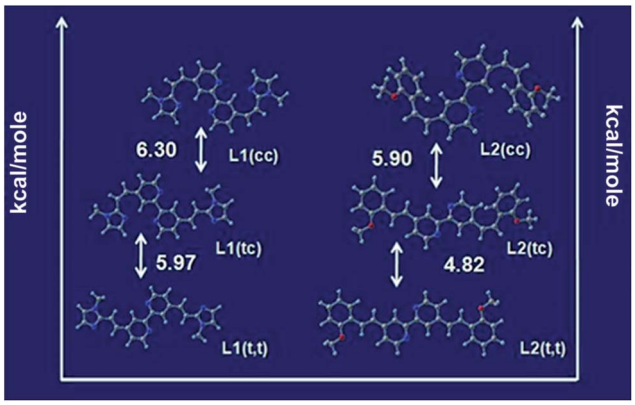

Fig. 10 The calculated energy difference between *trans–trans*, *trans–cis* and *cis–cis* geometrical forms of the ligands L1 and L2.

for 10minutes + gradient 50% to 100% (v/v) of acetonitrile for 20 minutes), containing 0.1% (v/v) of HCl. The retention time of the two peaks of complex **1** were $t = 9.53$ min and $t = 10.01$ min, whereas for complex **2**, only one peak at $t = 10.39$ min is observed (Fig. S6(B)†).[20]

Theoretical studies

The ground state optimization of the *trans–trans*, *trans–cis* and *cis–cis* isomers of ligands **L1** and **L2** by performing density functional theory (DFT) at the B3LYP/(6-31G**) level were done and the optimized structures with energy differences are shown in Fig. 10. The optimized geometries of *trans–cis* and *cis–cis* isomers provide quite clear insight of the energy differences between the isomers. The time-dependent density functional (TDDFT) calculations were done only with the *trans–trans* isomer.

The molecular and electronic structures of the complexes **1** and**2** were investigated by performing combined density functional theory (DFT) and time-dependent density functional (TDDFT) calculations at the B3LYP/(6-31G**)+LANL2DZ level. The calculations correctly reproduce the near-octahedral coordination of the metal centre observed in the X-ray structures and predicted geometric parameters are in good agreement with the X-ray structural data. Interestingly, the complex **2** always optimized in the $\mathbf{2_{final}}$ geometry. It implies that the stable geometry of the complex is depicted in the $\mathbf{2_{final}}$ state. Energies of the frontier molecular orbitals were determined and plots of the HOMO (HOMO to HOMO−3 for **L1**, **1**, **2** and HOMO to HOMO−4 for **L2**) and LUMO (LUMO to LUMO+1 for **L1**, **L2**, **1** and LUMO to LUMO+2 for **2**) orbitals for the ligands and the non-substituted $[Ir(ppy)_2(arylethenylbpy)]^+$ cation are depicted in Fig. 11.

The calculations help us to correlate the spectral data and assignment for the transitions accordingly. The lowest energy transition of the ligand **L1** has oscillator frequency (*f*) 1.6388 (>1) of **L1**, whereas it is slightly less than 1 in case of **L2** ($f = 0.9779$) (Table 2). It occurs especially on highly symmetric molecules.

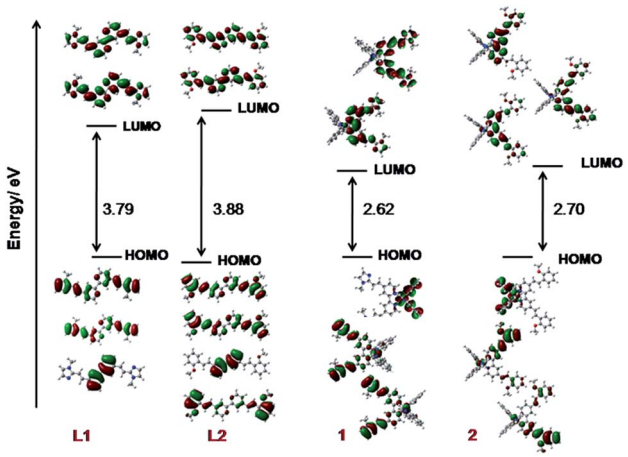

Fig. 11 Schematic representation showing the isovalue contours and energy differences between HOMO and LUMO calculated for the ligands L1, L2 and complexes 1, 2.

Since most of the transitions are forbidden, the *f*-strengths are concentrated on one main peak.[21] The spectral assignments are consistent with the findings of TDDFT calculations (Table 2, Fig. 11). The transition in the ligands are mostly π–π* based.[22] The lower energy transitions of the complexes are MLCT and LC based, and mostly π (ppy, bpy) and π*bpy are involved in both **1** and **2**. To gain insight into the photophysical properties of **1** and **2**, we optimized the geometry of the lowest-energy triplet excited state (T_1) by using the spin-unrestricted UB3LYP approach.[23] The excitation to T_1 involves electron promotion from the orbital with electron density residing on the ppy fragment to the ancillary bpy ligand. Both the complexes have a similar spin-density distribution, mainly localized on the C∩N ligands together with a small contribution (about 0.13 e) from iridium. Therefore, T_1 can be described as a cyclometalating-ligand-centered triplet state, with a small metal contribution (Table 4). From a simple visual analysis of the positions of the major transitions depicted in Fig. 12, it can be seen that the energies of the calculated transitions are in good agreement with the experimentally recorded spectra. The predominant ligand centered nature of the emitting T_1 state explains the well resolved vibronic structure of the luminescence spectra of the complexes (Fig. 9).

Summarily, the ligands **L1** and **L2** isomerize only in the presence of UV-light. The well-established mechanism for the *trans–cis* isomerization of stilbenes describes that the formation of a singlet excited state causes promotion of an electron from HOMO to LUMO which repopulates the ground state primarily

Table 4 Lowest triplet excited states calculated (gas phase) at the TD-DFT B3LYP/(LANL2DZ) level for complexes 1–2

Complex	State	*E* (eV)	Assignments
1	T_1	2.2911	^{3}MLCT, ^{3}LC
2	T_1	2.1964	^{3}MLCT, ^{3}LC

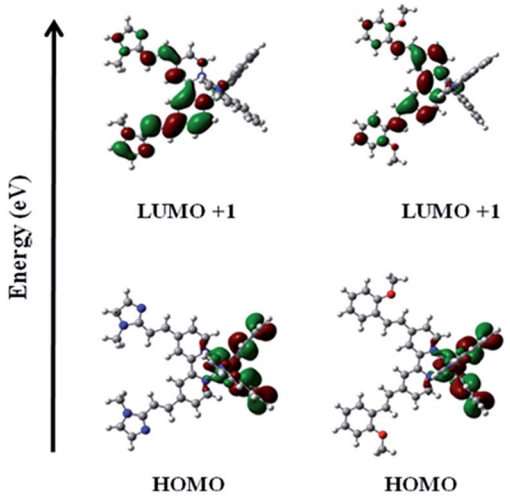

Fig. 12 Electron density contours calculated for the triplet emitting excited state (T_1) of **1** and **2** resulting from the HOMO-to-LUMO+1 monoexcitation (calculations were done in gas-phase).

in solution by isomerization to the *cis*-form.[9] At singlet excited state, the *trans*-form can twist around the central C=C bond orienting the planes perpendicular to both aryl rings to afford a mixture of *trans*- and *cis*-isomers. The isomerization process in the (aryl)ethenyl-functionalized bipyridyls possibly occurs exactly in the similar way. The calculation shows that for the free ligand the main transition is from HOMO−1 to LUMO+1 (~82 kcal mol^{-1}, HOMO–LUMO ~ 81.58 kcal mol^{-1}) in **L1** and to LUMO in **L2** (~85 kcal mol^{-1}, HOMO–LUMO ~ 94.75 kcal mol^{-1}). The rotational barrier for **L1** has been calculated around 8 kcal mol^{-1} (for **L2**, **1**, and **2**, it could not be calculated exactly, but of the same order) which is much lower than the excitation energy. The metal chelation, in contrast, populate the ^{1}MLCT and ^{3}LC, ^{3}MLCT state by means of internal conversion and intersystem crossing, compared to the free ligand as evident from the TDDFT calculation (Table 2, Fig. S13†). The energy released in the $T_1 \rightarrow S_o$ transition, is much less (~50 kcal mol^{-1}) compared to the ligand but definitely higher than the rotational barrier. Thus, *trans–cis* isomer formation from *trans–trans* variety is witnessed in the complexes. On a separate note, due to the bound character of the MLCT state, perpendicular intermediate formation is difficult. The difficulty in the formation of the transition state might be the reason for the restriction of isomerization of the chelated ligands in the complexes to only *trans–cis* isomerized state. The isomerization process is very slow in the ligands in presence of visible light. The presence of the low-lying MLCT states enables the photo-isomerization process to occur fast in the presence of visible light, in the chelated (aryl)ethenyl-functionalized bipyridyls.

Experimental section

Synthetic materials and methods

The starting materials $IrCl_3 \cdot 3H_2O$, 2-phenylpyridine, 4,4′-dimethyl-2,2′-bipyridine, and required aldehydes were purchased from Sigma-Aldrich and used without further purification. All the solvents were dried by usual methods prior to use. The cyclometalated iridium(III) chloro bridged dimer $[Ir(ppy)_2Cl]_2$ was prepared according to the literature methods.[24]

Synthesis of ligands

The synthesis of 4,4′-bis(diethylmethylphosphonate)-2,2′-bipyridine from the commercially available 4,4′-dimethyl-2,2′-bipyridine (1.84 g, 10.0 mmol) have been followed through five steps according to reported literature[25] and an off-white solid was obtained with 90% yield. The 4,4′-(aryl)ethenyl-substituted 2,2′-bipyridyls (**L1–L2**) have been synthesized by means of Horner–Wadsworth–Emmons coupling reactions: 4,4′-bis(diethylmethylphosphonate)-2,2′-bipyridine (0.2 mmol) in 20 mL of dry THF solution with the requisite aldehydes (0.5 mmol) (Scheme 1) in presence of ^{t}BuOK were stirred under dark condition for 2 h at room temperature. The reaction was quenched by the addition of 50 mL H_2O and stirred again for 10 min. The precipitate was filtered off and washed thoroughly with H_2O and air-dried. All ligands have been characterized by ^{1}H, ^{13}C NMR and mass spectrometry. The ESI-MS data of the ligands are shown in Fig. S13.†

L1. White solid. Yield: 72.7 mg (86.5%), ESI-MS: 369.18 (M^+). CHN: calc. C, 71.72; H, 4.42; N, 8.59, found C, 71.86; H, 4.63; N, 8.72. ^{1}H NMR (500 MHz, DMSO-d_6) δ (ppm) 8.70–8.69 (2H, d, J = 5.05 Hz); 8.55 (2H, s); 7.74–7.73 (2H, dd, J = 1.30 Hz, 5.05 Hz); 7.59–7.56 (2H, d, J = 15.75 Hz); 7.46–7.43 (2H, d, J = 15.75 Hz); 7.25 (2H, s); 7.02 (2H, s); 3.82 (6H, s). ^{13}C NMR (400 MHz, $CDCl_3$) δ (ppm) 155.92, 149.69, 145.05, 144.21, 128.86, 127.57, 123.28, 121.42, 119.39, 117.81, 32.53.

L2. White solid. Yield: 68.2 mg (81.2%), ESI-MS: 421.20 (M^+) CHN: calc. C, 79.98; H, 5.75; N, 6.66, found C, 79.84; H, 5.97; N, 6.72. ^{1}H NMR (500 MHz, DMSO-d_6) δ (ppm) 8.69–8.68 (2H, d, J = 5.05 Hz); 8.53 (2H, s); 7.78 (2H, s); 7.76–7.74 (2H, t, J = 5.02 Hz); 7.64–7.62 (2H, dd, J = 1.9 Hz, 1.55 Hz); 7.41–7.34 (4H, m); 7.11–7.10 (2H, d, J = 4.25 Hz); 7.04–7.01 (2H, t, J = 7.55 Hz); 3.91 (6H, s). ^{13}C NMR (500 MHz, $CDCl_3$) δ (ppm) 157.02, 155.68, 149.77, 145.83, 130.18, 127.60, 127.15, 126.55, 124.41, 121.12, 120.72, 117.37, 111.59, 55.60.

Synthesis of complexes

Complexes **1–2** (Scheme 1) were prepared by refluxing ligands **L1–L2** (0.22 mmol) with $[Ir(ppy)_2Cl]_2$ (107.2 mg, 0.1 mmol) in acetonitrile : dichloromethane (1 : 1) at 70 °C for 3 h under complete dark condition.[26] In both the cases red colored solution were obtained. The crude mixture was purified by thin layer chromatography using 5 : 1 dichloromethane–methanol as eluent to get the pure product. All the complexes have been characterized by ^{1}H, ^{13}C, ^{1}H–^{1}H COSY, ^{1}H–^{1}H NOESY, mass spectrometry, and CHN analysis. The ESI-MS and ^{13}C NMR data are shown in Fig. S14 and S10.†

$[Ir(ppy)_2(L1)]^+$ (1, *trans–trans*). Reddish-orange. Yield: 132.2 mg (69.1%). ESI-MS: 869.26 (M^+). CHN: calc. C, 58.43; H, 4.01; N, 12.39, found C, 58.59; H, 4.04; N, 12.51. ^{1}H NMR (500 MHz, DMSO-d_6) δ (ppm) 9.56 (2H, s); 8.27 (2H, d, J = 8.2 Hz); 8.21 (2H, d, J = 15.75 Hz); 7.95–7.92 (4H, t, J = 16.4 Hz); 7.84 (2H, d, J = 5.7 Hz); 7.74 (2H, t, J = 5.6 Hz); 7.71 (2H, d, J = 5.65 Hz); 7.47

(2H, d, $J = 15.75$ Hz); 7.29 (2H, s); 7.19 (2H, t, $J = 6.48$ Hz); 7.06 (2H, s); 7.01 (2H, t, $J = 7.55$ Hz); 6.91 (2H, t, $J = 7.4$ Hz); 6.22 (2H, d, $J = 7.55$ Hz); 3.90 (H4, 6H, s). ^{13}C NMR (400 MHz, $CDCl_3$) δ (ppm) 167.99, 156.39, 151.47, 149.83, 148.68, 148.41, 145.57, 143.43, 137.80, 131.71, 130.72, 129.66, 126.96, 126.20, 125.32, 124.75, 123.14, 123.03, 122.39, 122.25, 119.52, 34.46.

$[Ir(ppy)_2(L2)]^+$ (2, *trans–trans*). Red. Yield: 143.9 mg (75.2%). ESI-MS: 921.25 (M^+). CHN: calc. C, 62.78; H, 4.21; N, 5.86, found C, 62.98; H, 4.10; N, 5.92. ^{1}H NMR (400 MHz, $CDCl_3$) δ (ppm) 9.64 (2H, s); 7.99 (2H, d, $J = 16.8$ Hz); 7.92–7.88 (4H, 2d, $J = 6.88$ and 6.12 Hz); 7.77–7.72 (4H, 2d, 6.88 and 6.12 Hz); 7.68 (2H, d); 7.64 (2H, d, 16.8 Hz); 7.58 (2H, d, $J = 6.12$ Hz); 7.51 (d, $J = 6.12$ Hz); 7.29 (2H, d); 7.04–6.98 (6H, m); 6.93–6.86 (4H, q); 6.33 (2H, d, $J = 6.84$ Hz); 3.88 (6H, s). ^{13}C NMR (400 MHz, $CDCl_3$) δ (ppm) 167.95, 157.75, 156.42, 151.37, 149.62, 149.10, 148.49, 143.52, 137.84, 132.53, 131.78, 130.66, 130.53, 129.23, 124.89, 124.67, 124.57, 123.13, 123.04, 122.35, 121.13, 119.43, 110.76, 55.51.

Physical measurements

IR spectra were obtained on a Perkin-Elmer Spectrum RXI spectrophotometer with samples prepared as KBr pellets. Elemental analyses were performed on a Perkin-Elmer 2400 series II CHN series. Electronic spectra were recorded on a U-4100, HITACHI spectrometer. ^{1}H NMR spectra were obtained on a Bruker Avance III-500 NMR spectrometer using TMS as the internal standard. HPLC was done with Waters 600 HPLC system with CHIRALCEL OD-H column. Electrochemical measurements were made using a PAR model 273 potentiostat. A platinum disk working electrode, a platinum wire auxiliary electrode and an aqueous saturated calomel reference electrode (SCE) were used in a three electrode configuration. Electrochemical measurements were made under nitrogen atmosphere. Mass spectra were recorded on a Q-Tof-Micromass spectrometer by positive-ion mode electrospray ionization. Fluorescence spectra were taken on a HORIBA JOBINYVON spectrofluorimeter. Quantum yields were determined in CH_2Cl_2 with quinine sulfate in 0.1 M H_2SO_4 solution as a reference ($\Phi = 0.577$), and calculated with the following equation:

$$\Phi_{sample} = \Phi_{ref} \times \frac{I_{sample}}{I_{ref}} \times \frac{A_{ref}}{A_{sample}} \times \frac{{\eta_{sample}}^2}{{\eta_{ref}}^2}$$

Φ, I, A, η are quantum yield, integral emission intensity, absorbance and refractive index of the solvents respectively, in which the sample or reference was dissolved.

X-ray crystallography

Single crystal of **L1** and **L2** were crystallized from saturated DMSO solution and by slow evaporation of DCM solution, respectively. **2** and $\mathbf{2_{final}}$ were obtained by slow evaporation of DCM solution containing ammonium hexafluorophosphate and slow evaporation of chloroform solution of complex **1** yielded good quality crystals. Crystal data of the complexes were collected on a Bruker SMART APEXII CCD area-detector diffractometer using graphite monochromated Mo Kα radiation ($\lambda = 0.71073$ Å). For **L1** and **L2**, date were collected on a CrysAlis Pro, Super Nova, Eos four-circle diffractometer using mirror monochromated Mo Kα radiation ($\lambda = 0.71073$ Å). For crystals **L1** and **L2**, X-ray data reduction was carried out using the *CrysAlis PRO*, Agilent Technologies, Version 1.171.36.24 program and for the complexes, X-ray data reduction was carried out using the Bruker *SAINT* program. The structures were solved by direct methods using the SHELXS-97 program and refinement using SHELXL-97 program. Selected crystal data and data collection parameters for all the complexes are given in Table 3. X-ray structure solution and refinement were done using the SHELXL-97 program package.[27] Four final cycles of refinement converged with discrepancy indices $R[F^2 > 2\sigma(F^2)] = 0.0628$ and $wR(F^2) = 0.1457$ for **L1**, $R[F^2 > 2\sigma(F^2)] = 0.0539$ and $wR(F^2) = 0.1484$ for **L2**, $R[F^2 > 2\sigma(F^2)] = 0.0678$ and $wR_{F^2} = 0.1646$ for **1**, $R[F^2 > 2\sigma(F^2)] = 0.0701$ and $wR(F^2) = 0.1898$ for **2**, and $R[F^2 > 2\sigma(F^2)] = 0.0679$ and $wR(F^2) = 0.1428$ for $\mathbf{2_{final}}$.

Computational method

The ground-state geometry of the ligands and the complexes has been optimized in the absence of the counter-ion at the Density Functional Theory (DFT) level, using the X-ray structures. The basis set for the description of the electrons of nonmetallic atoms is B3LYP/6-31G, while for iridium the B3LYP/LANL2DZ basis set has been used. The characterization of the nature of the lowest-lying singlet and triplet excited states involved in absorption and emission properties, respectively, relies on time-dependent density functional theory (TD-DFT) calculations performed on the basis of the ground-state geometry, using the same basis set. All calculations were performed with the Gaussian09 package.[28]

Conclusions

We have synthesized two (aryl)ethenyl functionalized 2,2′-bipyridine and their iridium(III) complexes. We report the dynamic photophysical properties of these cyclometalated Ir(III) complexes with detail analysis of spectroscopic and spectrophotometric characterizations. In addition, quantum chemical calculation rationalizes the experimental observations of the anomalous photoinduced behavior of complexes **1** and **2**. To the best of our knowledge, this is the first report of detail study for photophysical properties of these cyclometalated iridium(III) complexes to investigate the mechanism of photoinduced *trans–cis* isomerism. The *trans–cis* photoisomerization mechanism in the ligands involve singlet excited state, whereas the iridium(III) complexes of the same ligands involves low lying ^{3}MLCT state. This is expected from the above observations that a careful choice of the substituted (aryl)ethenyl appended bipyridyl ligands in the cyclometalated Ir(III) complexes could prevent the isomerization process completely. The selectivity of photoinduced isomers might have crucial importance in development of cyclometalated iridium(III) complexes for applications in photochromic systems.

Acknowledgements

Soumalya Sinha and Soumik Mandal are thankful to KVPY and CSIR, New Delhi for their Fellowship. This work is supported by DST, New Delhi through research grants ST/FT/CS-057/2009 awarded to Parna Gupta.

References

1 (*a*) V. W.-W. Yam and K. M.-C. Wo, *Chem. Commun.*, 2011, **47**, 11579; (*b*) Y. You, S. Cho and W. Nam, *Inorg. Chem.*, 2014, **53**, 1804; (*c*) M. Marín-Suárez, B. F. E. Curchod, I. Tavernelli, U. Rothlisberger, R. Scopelliti, I. Jung, D. D. Censo, M. Grätzel, J. F. Fernández-Sánchez, A. Fernández-Gutiérrez, M. K. Nazeeruddin and E. Baranoff, *Chem. Mater.*, 2012, **24**, 2330; (*d*) M. S. Lowry and S. Bernhard, *Chem.–Eur. J.*, 2006, **12**, 7970; (*e*) L. Flamigni, J. Collin and J. Sauvage, *Acc. Chem. Res.*, 2008, **41**, 857.

2 (*a*) C.-H. Chang, Z.-J. Wu, C.-H. Chiu, Y.-H. Liang, Y.-S. Tsai, J.-L. Liao, Y. Chi, H.-Y. Hsieh, T.-Y. Kuo, G.-H. Lee, H.-A. Pan, P.-T. Chou, J.-S. Lin and M.-R. Tseng, *ACS Appl. Mater. Interfaces*, 2013, **5**, 7341; (*b*) Y. Chi and P. T. Chou, *Chem. Soc. Rev.*, 2010, **39**, 638; (*c*) C.-H. Lin, Y.-Y. Chang, J.-Y. Hung, C.-Y. Lin, Y. Chi, M.-W. Chung, C.-L. Lin, P.-T. Chou, G.-H. Lee, C.-H. Chang and W.-C. Lin, *Angew. Chem., Int. Ed.*, 2011, **50**, 3182; (*d*) H. Cao, G. Shan, X. Wen, H. Sun, Z. Su, R. Zhong, W. Xie, P. Li and D. Zhu, *J. Mater. Chem. C*, 2013, **1**, 7371; (*e*) F. Kessler, Y. Watanabe, H. Sasabe, H. Katagiri, M. K. Nazeeruddin, M. Grätzel and J. Kido, *J. Mater. Chem. C*, 2013, **1**, 1070; (*f*) C. Wu, H.-F. Chen, K.-T. Wong and M. E. Thompson, *J. Am. Chem. Soc.*, 2010, **132**, 3133; (*g*) S. Lamansky, P. Djurovich, D. Murphy, F. Abdel-Razzaq, H.-E. Lee, C. Adachi, P. E. Burrows, S. R. Forrest and M. E. Thompson, *J. Am. Chem. Soc.*, 2001, **123**, 4304; (*h*) F.-C. Chen, Y. Yang, M. E. Thompson and J. Kido, *Appl. Phys. Lett.*, 2002, **80**, 2308; (*i*) H. J. Bolink, E. Coronado, S. G. Santamaria, M. Sessolo, N. Evans, C. Klein, E. Baranoff, K. Kalyanasundaram, M. Grätzel and M. K. Nazeeruddin, *Chem. Commun.*, 2007, 3276; (*j*) E. Baranoff, B. F. E. Curchod, J. Frey, R. Scopelliti, F. Kessler, I. Tavernelli, U. Rothlisberger, M. Grätzel and M. K. Nazeeruddin, *Inorg. Chem.*, 2012, **51**, 215.

3 (*a*) A. C. Brooks, K. Basore and S. Bernhard, *Inorg. Chem.*, 2013, **52**, 5794; (*b*) X. Yang, N. Sun, J. Dang, Z. Huang, C. Yao, X. Xu, C.-L. Ho, G. Zhou, D. Ma, X. Zhao and W.-Y. Wong, *J. Mater. Chem. C*, 2013, **1**, 3317; (*c*) C. Rothe, C.-J. Chiang, V. Jankus, M. R. Bryce, X. Zeng and A. P. Monkman, *Adv. Funct. Mater.*, 2009, **19**, 2038; (*d*) X. Zeng, M. Tavasli, A. S. Batsanov, M. R. Bryce, C.-J. Chiang, C. Rothe and A. P. Monkman, *Chem.–Eur. J.*, 2008, **14**, 933; (*e*) J. Zhang, L. Zhou, H. A. Al-Attar, K. Shao, L. Wang, D. Zhu, Z. Su, M. R. Bryce and A. P. Monkman, *Adv. Funct. Mater.*, 2013, **23**, 4667; (*f*) D. Tordera, J. J. Serrano-Perez, A. Pertegas, E. Orti, H. J. Bolink, E. Baranoff, M. K. Nazeeruddin and J. Frey, *Chem. Mater.*, 2013, **25**, 3391.

4 Y. You and W. Nam, *Chem. Soc. Rev.*, 2012, **41**, 7061.

5 (*a*) P. N. Curtin, L. L. Tinker, C. M. Burgess, E. D. Cline and S. Bernhard, *Inorg. Chem.*, 2009, **48**, 10498; (*b*) L. L. Tinker, N. D. McDaniel, P. N. Curtin, C. K. Smith, M. J. Ireland and S. Bernhard, *Chem.–Eur. J.*, 2007, **13**, 8726; (*c*) R. Lalrempuia, N. D. McDaniel, H. Müller-Bunz, S. Bernhard and M. Albrecht, *Angew. Chem., Int. Ed.*, 2010, **49**, 9765; (*d*) S. Metz and S. Bernhard, *Chem. Commun.*, 2010, **46**, 7551.

6 (*a*) E. Baranoff, J.-H. Yum, I. Jung, R. Vulcano, M. Grätzel and M. K. Nazeeruddin, *Chem.–Asian J.*, 2010, **5**, 496; (*b*) E. I. Mayo, K. Kilså, T. Tirrell, P. I. Djurovich, A. Tamayo, M. E. Thompson, N. S. Lewis and H. B. Gray, *Photochem. Photobiol. Sci.*, 2006, **5**, 871; (*c*) C. Dragonetti, A. Valore, A. Colombo, S. Righetto and V. Trifiletti, *Inorg. Chim. Acta*, 2012, **388**, 163; (*d*) Y.-J. Yuan, J.-Y. Zhang, Z.-T. Yu, J.-Y. Feng, W.-J. Luo, J.-H. Ye and Z.-G. Zou, *Inorg. Chem.*, 2012, **51**, 4123; (*e*) Y. Shinpuku, F. Inui, M. Nakai and Y. Nakabayashi, *J. Photochem. Photobiol., A*, 2011, **222**, 203.

7 (*a*) H. Huo, C. Fu, K. Harms and E. Meggers, *J. Am. Chem. Soc.*, 2014, **136**, 2990; (*b*) G. Choi, H. Tsurugi and K. Mashima, *J. Am. Chem. Soc.*, 2013, **135**, 13149; (*c*) O. F. Jeker, A. G. Kravina and E. M. Carreira, *Angew. Chem., Int. Ed.*, 2013, **52**, 12166; (*d*) D. A. Nagib, M. E. Scott and D. W. C. MacMillan, *J. Am. Chem. Soc.*, 2009, **131**, 10875; (*e*) J. A. Terrett, M. D. Clift and D. W. C. MacMillan, *J. Am. Chem. Soc.*, 2014, **136**, 6858; (*f*) J. Y. Hamilton, D. Sarlah and E. M. Carreira, *J. Am. Chem. Soc.*, 2014, **136**, 3006; (*g*) A. Noble and D. W. C. MacMillan, *J. Am. Chem. Soc.*, 2014, **136**, 11602.

8 (*a*) R.-D. Costa, F. Monti, G. Accorsi, A. Barbieri, H.-J. Bolink, E. Ortí and N. Armaroli, *Inorg. Chem.*, 2011, **50**, 7229; (*b*) V. Aubert, L. Ordronneau, M. Escadeillas, J. A. G. Williams, A. Boucekkine, E. Coulaud, C. Dragonetti, S. Righetto, D. Roberto, R. Ugo, A. Valore, A. Singh, J. Zyss, I. L. Rak, H. le Bozec and V. Guerchais, *Inorg. Chem.*, 2011, **50**, 5027; (*c*) P. Zhang, P.-A. Jacques, M. C. Kerlidou, M. Wang, L. Sun, M. Fontecave and V. Artero, *Inorg. Chem.*, 2012, **51**, 2115; (*d*) D. N. Chirdon, C. E. McCusker, F. N. Castellano and S. Bernhard, *Inorg. Chem.*, 2013, **52**, 8795; (*e*) Y. Yang, Q. Zhao, W. Feng and F. Li, *Chem. Rev.*, 2013, **113**, 192; (*f*) K. L. Haas and K. J. Franz, *Chem. Rev.*, 2009, **109**, 4921; (*g*) F. Neve, A. Crispini, S. Campagna and S. Serroni, *Inorg. Chem.*, 1999, **38**, 2250.

9 (*a*) E. V. Tulyakova, G. Vermeersch, E. N. Gulakova, O. A. Fedorova, Y. V. Fedorov, J. C. Micheau and S. P. Delbaere, *Chem.–Eur. J.*, 2010, **16**, 5661; (*b*) M. Mac, A. Danel, T. Uchacz, S. Gorycka, K. Górz, S. Lésniewski and E. Kulig, *Photochem. Photobiol. Sci.*, 2010, **9**, 357; (*c*) G. Orlandi and G. C. Marconi, *Chem. Phys.*, 1975, **8**, 458; (*d*) D. H. Waldeck, *Chem. Rev.*, 1991, **91**, 415; (*e*) H. Goerner and H. Kuhn, *Adv. Photochem.*, 1995, **19**, 1.

10 (*a*) H. Kang, A. Facchetti, H. Jiang, E. Cariati, S. Righetto, R. Ugo, C. Zuccaccia, A. Macchioni, C. L. Stern, Z. Liu, S.-T. Ho, E. C. Brown, M. A. Ratner and T. J. Marks, *J. Am. Chem. Soc.*, 2007, **129**, 3267; (*b*) B. J. Coe, J. A. Harris, B. S. Brunschwig, J. Garin, J. Orduna, S. J. Coles and

M. B. Hursthouse, *J. Am. Chem. Soc.*, 2004, **126**, 10418; (*c*) C. Feuvrie, O. Maury, H. Le Bozec, I. Ledoux, J. P. Morrall, G. T. Dalton, M. Samoc and M. G. Humphrey, *J. Phys. Chem. A*, 2007, **111**, 8980; (*d*) C. K. Chiang, C. R. Fincher Jr, Y. W. Park, A. J. Heeger, H. Shirakawa, E. J. Louis, S. C. Gau and A. G. MacDiarmid, *Phys. Rev. Lett.*, 1977, **39**, 1098; (*e*) Y.-Y. Lin, D. J. Gundlach, S. Nelson and T. N. Jackson, *IEEE Electron Device Lett.*, 1997, **18**, 606; (*f*) C. A. Stanier, S. J. Alderman, T. D. W. Claridge and H. L. Anderson, *Angew. Chem., Int. Ed.*, 2002, **41**, 1769; (*g*) E. W. Debler, G. F. Kaufmann, M. M. Meijler, A. Heine, J. M. Mee, G. Pljevaljčić, A. J. Di Bilio, P. G. Schultz, D. P. Millar, K. D. JandavI, A. Wilson, H. B. Gray and R. A. Lerner, *Science*, 2008, **319**, 1232; (*h*) U. Mitschke and P. J. Bäuerle, *J. Mater. Chem.*, 2000, **10**, 1471; (*i*) R. H. Friend, R. W. Gymer, A. B. Holmes, J. H. Burroughes, R. N. Marks, C. Taliani, D. D. C. Bradley, D. A. D. Santos, J. L. Brédas, M. Lögdlund and W. R. Salaneck, *Nature*, 1999, **397**, 121; (*j*) A. Colombo, C. Dragonetti, D. Marinotto, S. Righetto, D. Roberto, S. Tavazzi, M. Escadeillas, V. G. uerchais, H. le Bozec, A. Boucekkine and C. Latouche, *Organometallics*, 2013, **32**, 3890; (*k*) M. Chandrasekharam, T. Suresh, S. P. Singh, B. Priyanka, K. Bhanuprakash, A. Islam, L. Hanb and M. K. Lakshmi, *Dalton Trans.*, 2012, **41**, 8770; (*l*) F. Gajardo, M. Barrera, R. Vargas, I. Crivelli and B. Loeb, *Inorg. Chem.*, 2011, **50**, 5910.

11 (*a*) C. Baik and S. Wang, *Chem. Commun.*, 2011, **47**, 9432; (*b*) C. Baik, Z. M. Hudson, H. Amarne and S. Wang, *J. Am. Chem. Soc.*, 2009, **131**, 14549.

12 (*a*) F. Nisic, A. Colombo, C. Dragonetti, D. Roberto, A. Valore, J. M. Malicka, M. Cocchi, G. R. Freemane and J. A. G. Williams, *J. Mater. Chem. C*, 2014, **2**, 1791; (*b*) H. Nitadori, L. Ordronneau, J. Boixel, D. Jacquemin, A. Boucekkine, A. Singh, M. Akita, I. Ledoux, V. Guerchais and H. Le Bozec, *Chem. Commun.*, 2012, **48**, 10395; (*c*) A. Grabulosa, D. Martineau, M. Beley, P. C. Gros, S. Cazzanti, S. Caramori, A. Carlo and C. A. Bignozzi, *Dalton Trans.*, 2009, 63; (*d*) B. Yin, F. Niemeyer, J. A. G. Williams, J. Jiang, A. Boucekkine, L. Toupet, H. Le Bozec and V. Guerchais, *Inorg. Chem.*, 2006, **45**, 8584.

13 J. D. Lewis, R. N. Perutz and N. J. Moore, *Chem. Commun.*, 2000, 1865.

14 (*a*) B. S. Furniss, A. J. Hannaford, P. W. G. Smith and A. R. Tatchell, *Vogel's Textbook of Practical Organic Chemistry*, Harlow Longman, 5th edn, 1989, vol. 69, ISBN 0-582-46236-3; (*b*) V. Aubert, V. Guerchais, E. Ishow, K. Hoang-Thi, I. Ledoux, K. Nakatani and H. Le Bozec, *Angew. Chem., Int. Ed.*, 2008, **47**, 577; (*c*) L. Ordronneau, H. Nitadori, I. Ledoux, A. Singh, J. A. G. Williams, M. Akita, V. Guerchais and H. Le Bozec, *Inorg. Chem.*, 2012, **51**, 5627.

15 F. P. Gasparro and N. H. J. Kolodny, *J. Chem. Educ.*, 1977, **54**, 258.

16 Q. Zhao, S. Liu, M. Shi, F. Li, H. Jing, T. Yi and C. Huang, *Organometallics*, 2007, **26**, 5922.

17 S. Ladouceur and E. Zysman-Colman, *Eur. J. Inorg. Chem.*, 2013, 2985.

18 (*a*) L. Flamigni, A. Barbieri, C. Sabatini, B. Ventura and F. Barigelletti, *Top. Curr. Chem.*, 2007, **281**, 143; (*b*) J. A. G. Williams, A. J. Wilkinson and V. L. Whittle, *Dalton Trans.*, 2008, 2081.

19 The peak positions remain the same when excited at 410 or 480 nm.

20 M. Felici, P. Contreras-Carballada, J. M. M. Smits, R. J. M. Nolte, R. M. Williams, L. D. Cola and M. C. Feiters, *Molecules*, 2010, **15**, 2039.

21 P. Limão-Vieira, K. Anzai, H. Kato, M. Hoshino, F. Ferreira da Silva, D. Duflot, D. Mogi, T. Tanioka and H. Tanaka, *J. Phys. Chem. A*, 2012, **116**, 10529.

22 D. Berner, C. Klein, Md. K. Nazeeruddin, F. de Angelis, M. Castellani, P. Bugnon, R. Scopelliti, L. Zuppirolid and M. Grätzel, *J. Mater. Chem.*, 2006, **16**, 4468.

23 C. E. Welby, L. Gilmartin, R. R. Marriott, A. Zahid, C. R. Rice, E. A. Gibson and P. I. P. Elliott, *Dalton Trans.*, 2013, **42**, 13527.

24 M. Nonoyama, *Bull. Chem. Soc. Jpn.*, 1974, **47**, 767.

25 I. Gillaizeau-Gauthier, F. Odobel, M. Alebbi, R. Argazzi, E. Costa, C. A. Bignozzi, P. Qu and G. J. Meyer, *Inorg. Chem.*, 2001, **40**, 6073.

26 S. Sprouse, K. A. King, P. J. Spellane and R. J. Watts, *J. Am. Chem. Soc.*, 1984, **106**, 6647.

27 G. M. Sheldrick, *Acta Crystallogr., Sect. B: Struct. Sci.*, 2008, **A64**, 112.

28 M. J. Frisch, G. W. Trucks, H. B. Schlegel, G. E. Scuseria, M. A. Robb, J. R. Cheeseman, G. Scalmani, V. Barone, B. Mennucci, G. A. Petersson, H. Nakatsuji, M. Caricato, X. Li, H. P. Hratchian, A. F. Izmaylov, J. Bloino, G. Zheng, J. L. Sonnenberg, M. Hada, M. Ehara, K. Toyota, R. Fukuda, J. Hasegawa, M. Ishida, T. Nakajima, Y. Honda, O. Kitao, H. Nakai, T. Vreven, J. A. Montgomery Jr, J. E. Peralta, F. Ogliaro, M. Bearpark, J. J. Heyd, E. Brothers, K. N. Kudin, V. N. Staroverov, R. Kobayashi, J. Normand, K. Raghavachari, A. Rendell, J. C. Burant, S. S. Iyengar, J. Tomasi, M. Cossi, N. Rega, J. M. Millam, M. Klene, J. E. Knox, J. B. Cross, V. Bakken, C. Adamo, J. Jaramillo, R. Gomperts, R. E. Stratmann, O. Yazyev, A. J. Austin, R. Cammi, C. Pomelli, J. W. Ochterski, R. L. Martin, K. Morokuma, V. G. Zakrzewski, G. A. Voth, P. Salvador, J. J. Dannenberg, S. Dapprich, A. D. Daniels, O. Farkas, J. B. Foresman, J. V. Ortiz, J. Cioslowski, and D. J. Fox, *Gaussian 09, Revision A.02*, Gaussian, Inc., Wallingford CT, 2009.